Supplementary Information Text

Previous research, sediment coring and topography

A first field campaign revealed the potential of the marsh deposits for palaeoenvironmental research (Supplementary Figures S1, S2) and confirmed the absence of an inner harbor at the bottom of the Minoan town[31], contrary to what had been assumed (Supplementary Reference S1). On this initial exploration, core C6 was the only one that left open the hypothesis of erosion of the marshy deposits by the Minoan tsunami. Unfortunately, the sand deposits above the erosional contact were lost and could not be analyzed but the erosion of the marshy deposits was clear. We obtained permission in 2015 to proceed with a new core drilling survey in the archaeological area to complement the previous one.

Methods

AMS Radiocarbon dating

The radiocarbon dates were performed in three laboratories (Lyon, Poznan and Beta-Analytic). Of the 50 dates obtained, 5 were rejected due to their inverse stratigraphic position and their inconsistency with the age-depth models (in italic, Tab. S1). They were mainly provided by millimeter-sized charcoals that have migrated in soil profiles as a result of post-depositional processes (2 dates) and two very small fragments of plants too young that probably correspond to reed rootlets (2 dates). Additionally, for the radiocarbon dates obtained from marine samples provided by other studies, we estimate the age reservoir for Mediterranean Sea and the ΔR from the Marine Reservoir Correction Database of Calib. 8.20. For the Aegean Sea we use a ΔR of -48±78 resulting from the average of the two sites available (Supplementary Reference S2) and for the Caesarea, we use -139±73 resulting from the average of the six nearest data available (< 40km, Supplementary Reference S3). Age-depth modelling was performed using Bacon 2.5.1. (Supplementary Figures S3 to S5) (Supplementary Reference S4). Combined dates were obtained using Oxcal R-combine function[49] (Supplementary Figures S6 to S8)

Sedimentological and geochemical analyses

Grain-Size Measurements

Organic matter was removed from the samples using hydrogen peroxide (35%). Sediment samples were dispersed with hexametaphosphate sodium (5‰). The grain size distribution (ranging from 0.04 to 2000µm) was measured by laser diffraction with a Beckman-Coulter LS230. Grain size of coarse material (>2mm) was determined using sieves ranging from 2 to 12mm.

Scanning X-Ray fluorescence spectrometry (XRF)

Core-scanner XRF measurements have been performed in two different laboratories. Measurements were done every 5mm for C30 and C26 (Fig. S10, S11) at EDYTEM (CNRS-University of Savoie Mont Blanc) and every 10mm for C21 at EPOC (CNRS-University of Bordeaux). In both cases, an X-Ray beam was generated with a rhodium anode and a 125µm beryllium window, which allows a voltage range from 7 to 50 kV and a current range of 0 to 2 mA. The analytical settings were adjusted at 10 kV and 1 mA to detect light elements and trace elements (*i.e.* Sr, Rb, Zr, Br, Pb, Cu) were detected in a second run, performed at 30 kV for 0.75 mA. Each measurement is expressed in counts per second (cps).

Results

Fig. S1. Geographical context of the palaeoenvironmental investigations at Malia. Photo of the Malia marsh and the Minoan town of Malia (©L. Lespez).

Fig. S2. Geomorphological map and location of the core drillings obtained in the Malia marsh.
1. Current coastal line (blue) and contour line (grey, 1m eq., main contour line (eq. 5m) bold grey); 2. Streams and ditch: intermittent (dashed line) and perennial flow (solid line); 3. Cretaceous limestone (Sidheropetra); 4. Pleistocene silty deposits; 5. Pleistocene calcarenite; 6. Beach barrier sand; 7. Sandy marshy deposits; 8. Marshy deposits; 9. Colluvial and fluvial deposits; 10. Core drillings 2015 (red dot), ante 2015 (green dot). Edited in Adobe Illustrator CS6 version 16.0.

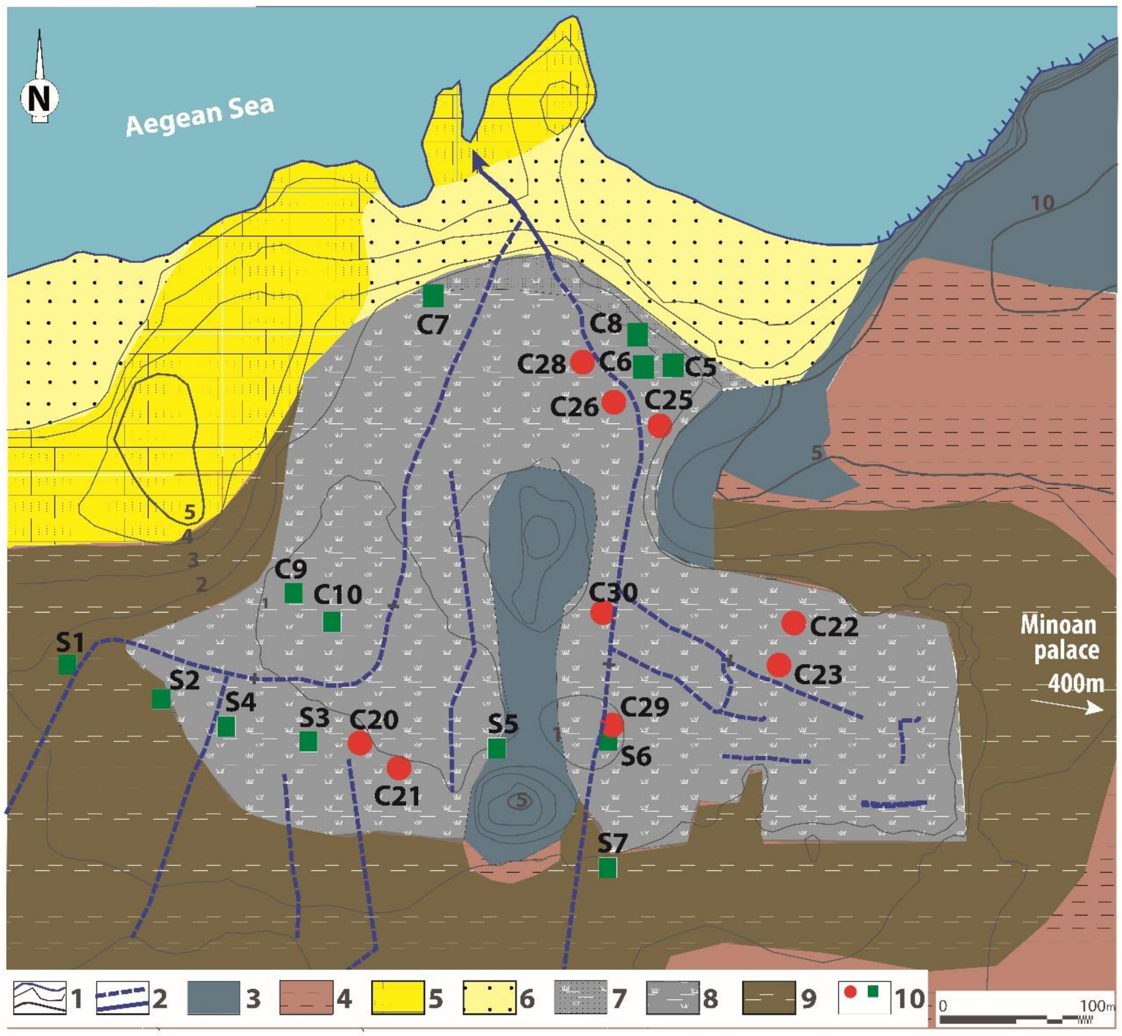

Fig. S3. Age-depth model of C21 core. Age-depth modelling was performed using Bacon 2.5.1 and radiocarbon dates from Table S1.

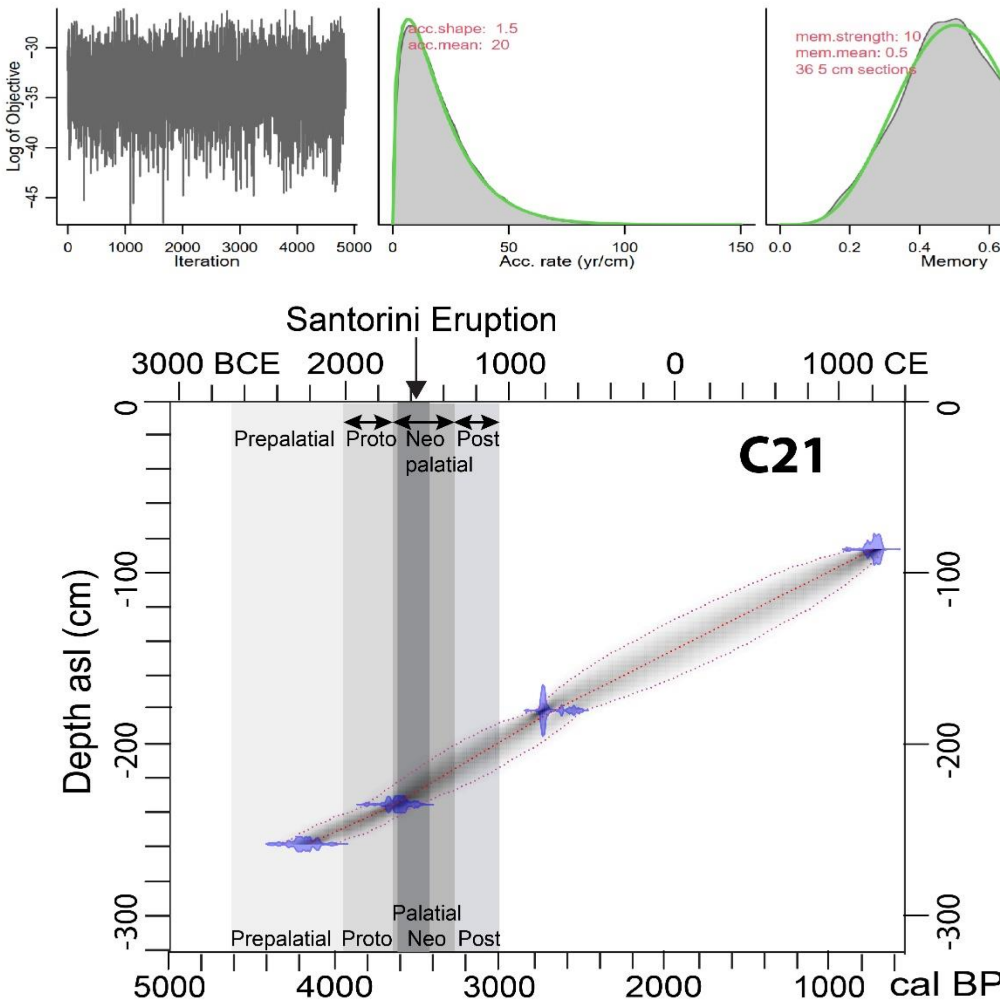

Fig. S4. Age-depth model of C6 core. Age-depth modelling was performed using Bacon 2.5.1 and radiocarbon dates from Table S1.

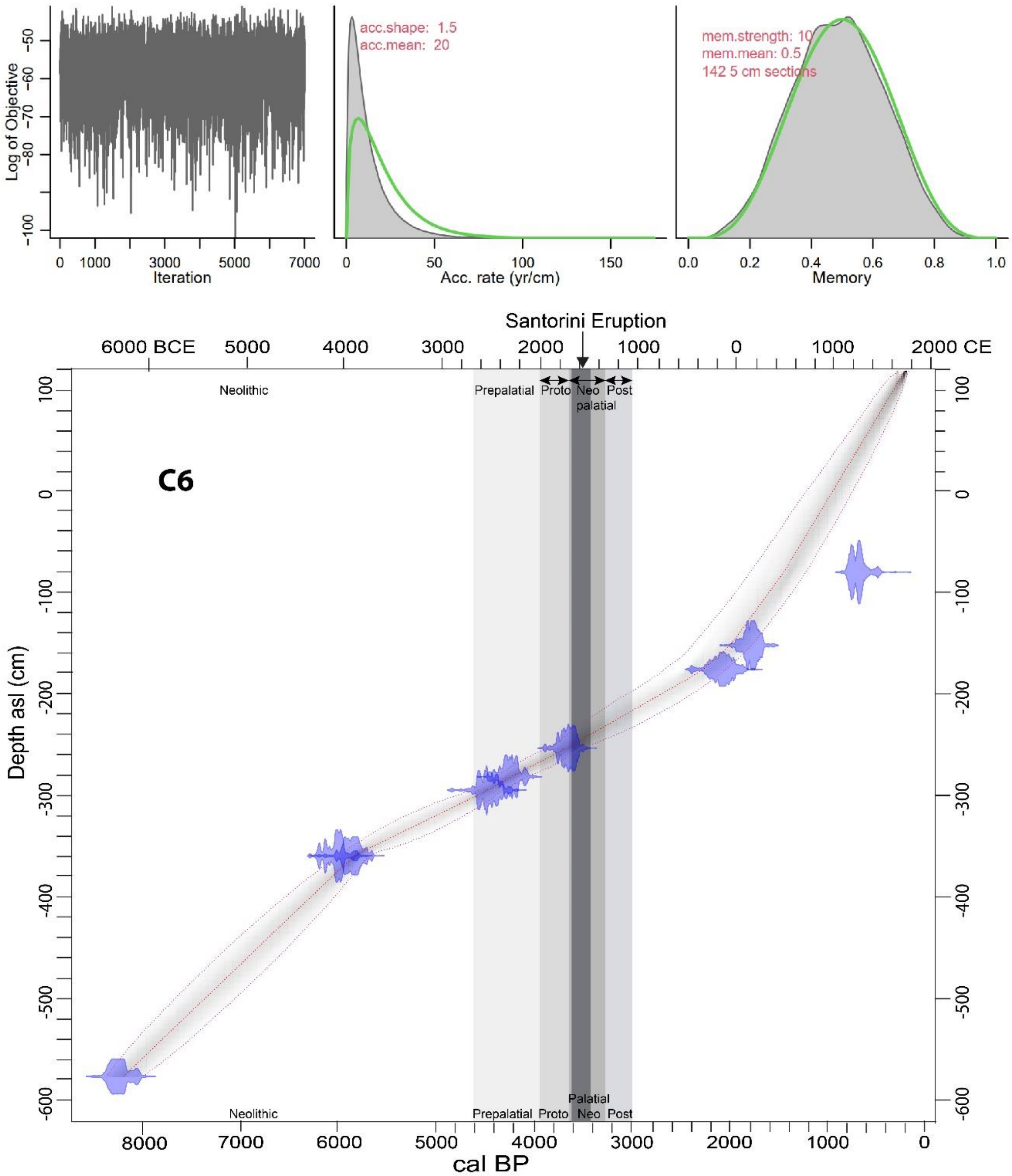

Fig. S5. Age-depth model of C26 core. Age-depth modelling was performed using Bacon 2.5.1 and radiocarbon dates from Table S1.

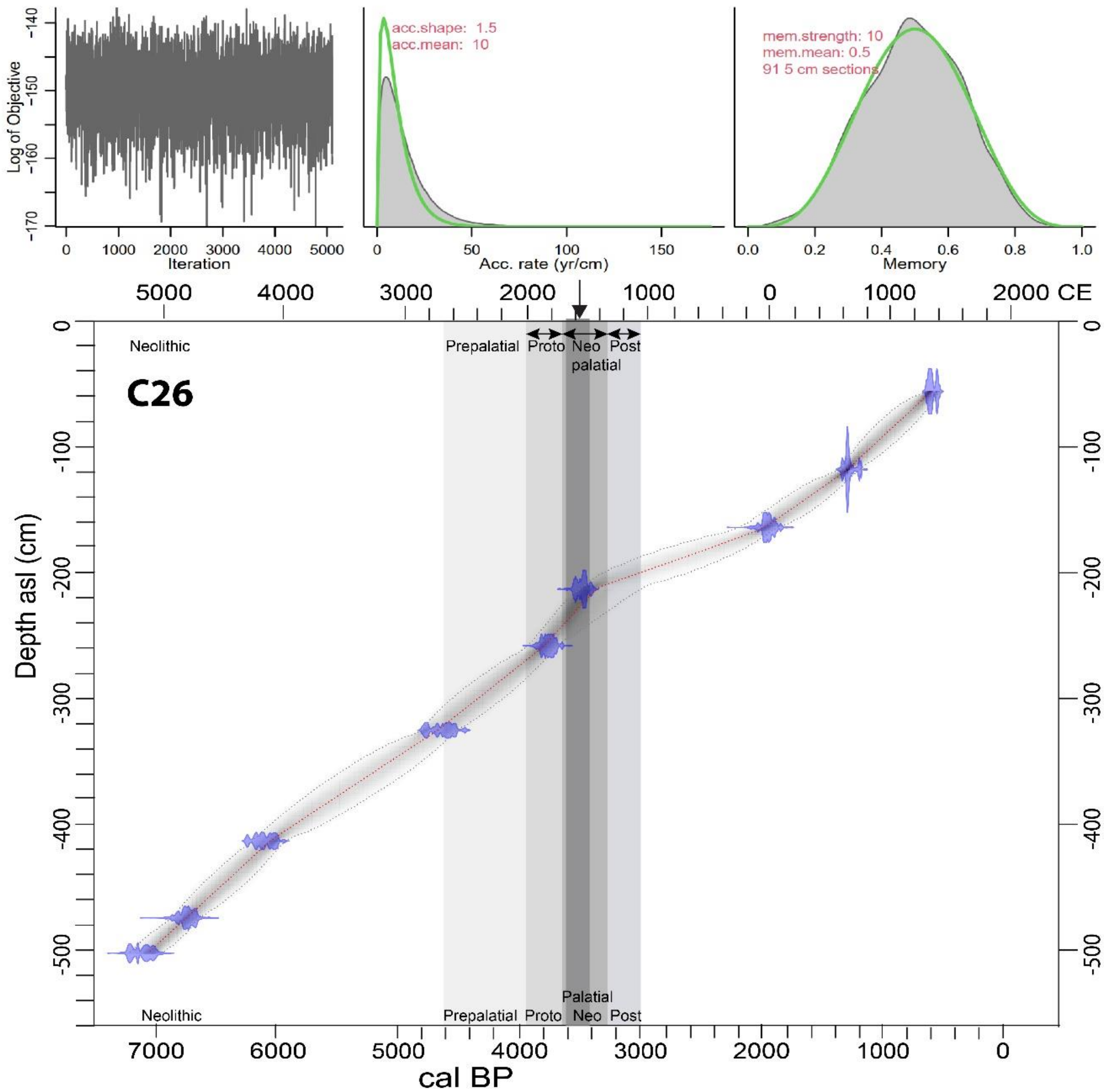

Fig. S6. Pre-tsunami combines dates. From C6 (3.755m), 3340 +/- 50 (Lyon-7116), and C21 (3.44m) 3380 +/-35 (Poz 95778).

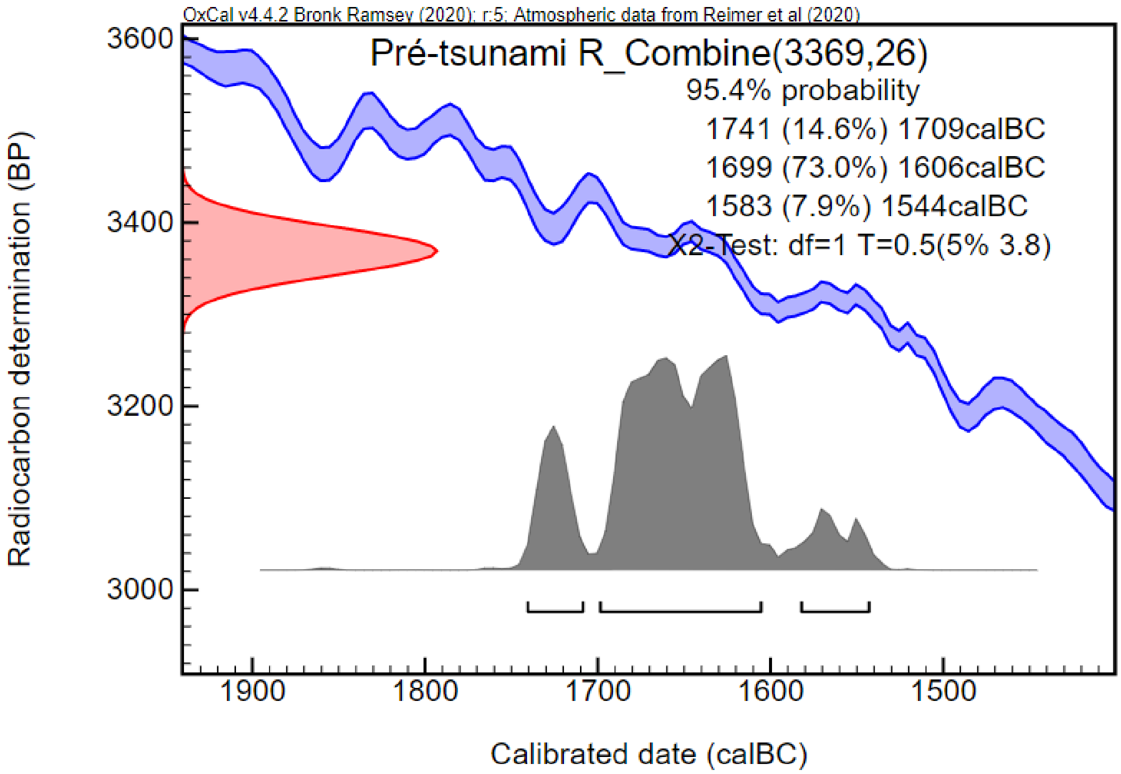

Fig. S7. Post-tsunami combines dates. From C20 (2.67m), 3220 +/- 30 (Poz-85442), and C22 (2.11m) 3200 +/-30 (Poz 96175).

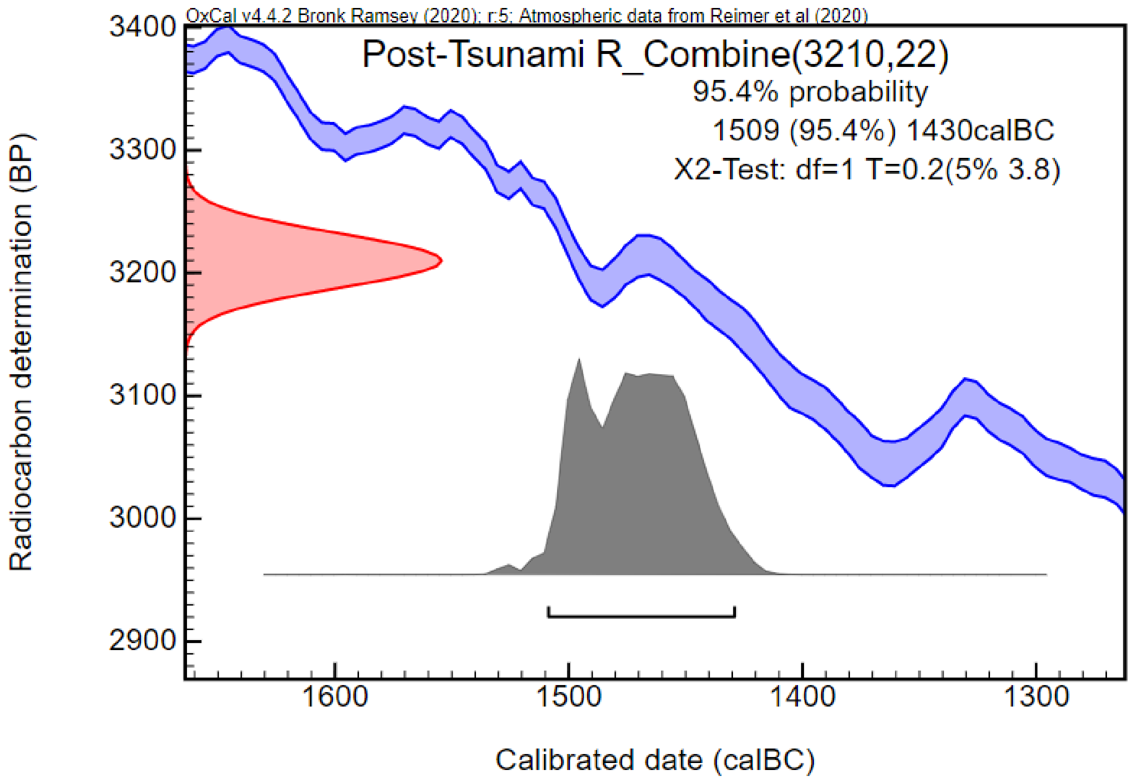

Fig. S8. R-combine Oxcal Gölhisar underlying tephra layers (dates in Eastwood et al., 1999)

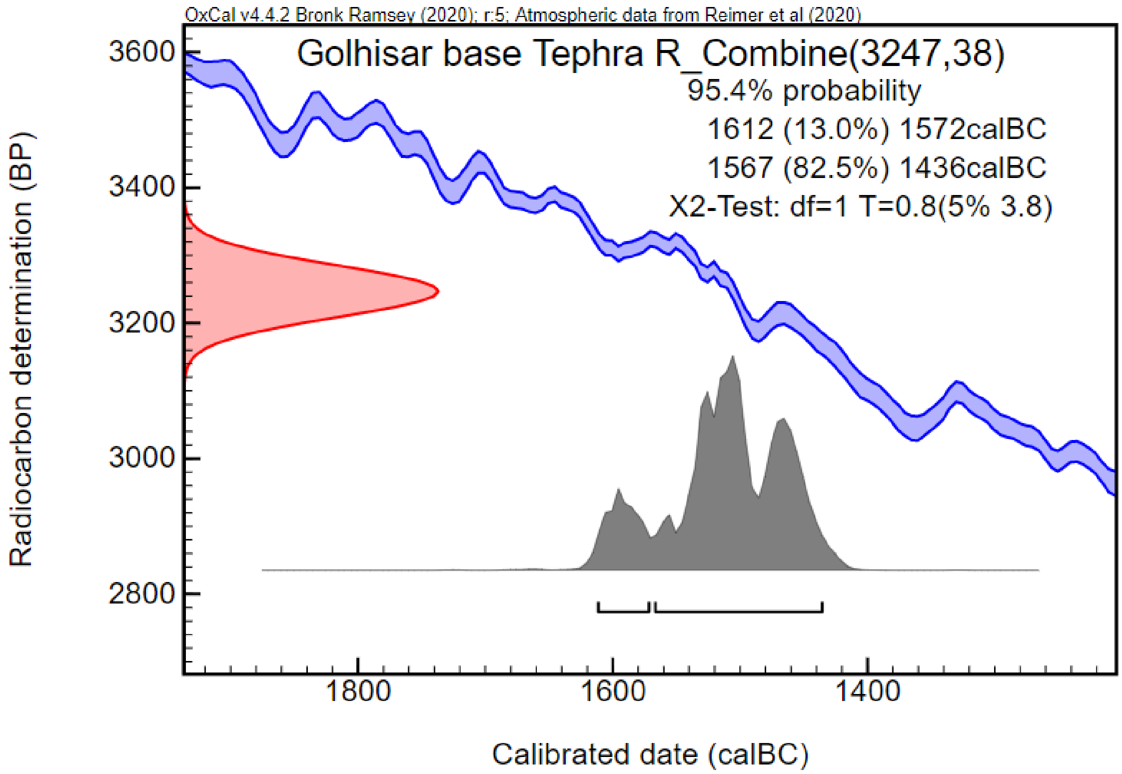

Fig. S9. C26 core selected analyses with radiocarbon sampling locations (black boxes), grain size, magnetic susceptibility and selection of major elements and geochemical ratios of clastic sources, carbonate content and redox conditions obtained from XRF core scanner analyses. 1. Sand. 2. Red-ochre Pleistocene silt; 3. Dark grey organic silt; 4. Brown silt.

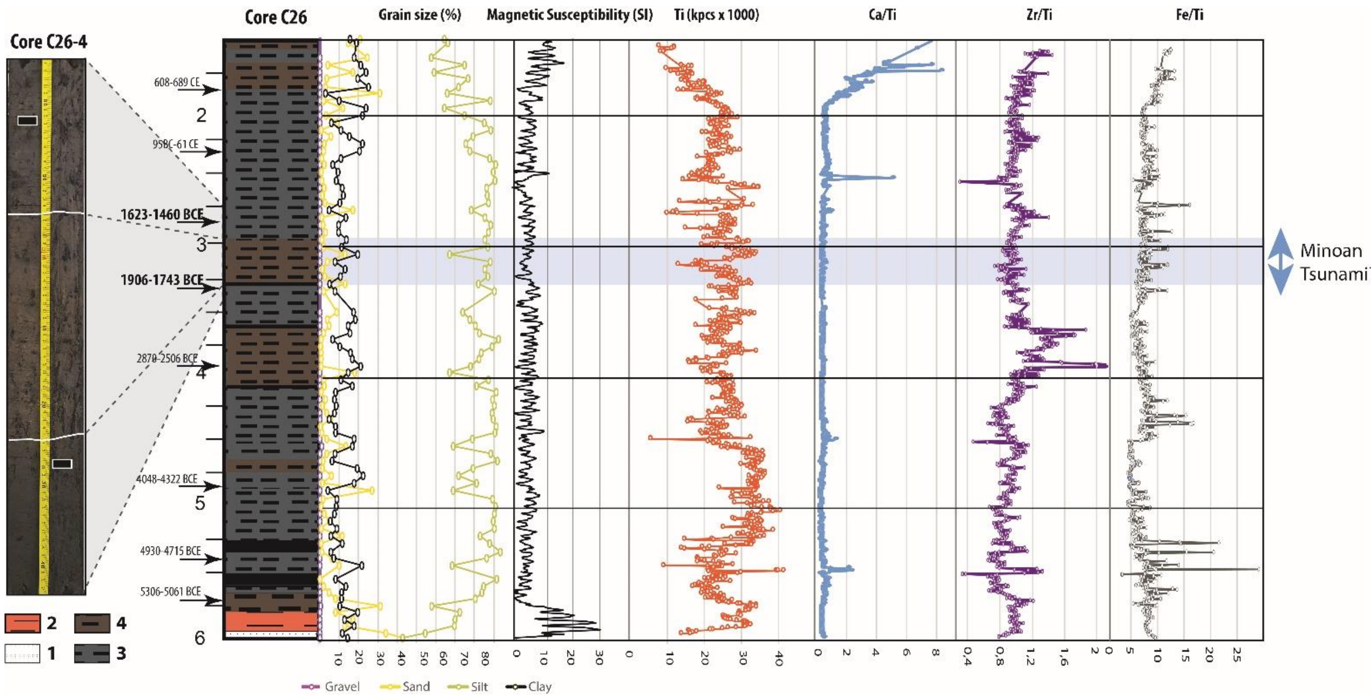

Fig. S10. C30 core selected analyses with selected analyses with radiocarbon sampling locations (black boxes), grain size, magnetic susceptibility and selection of major elements and geochemical ratios of clastic sources, carbonate content and redox conditions obtained from XRF core scanner analyses. 1. Dark grey organic silt. 2. Brown silt; 3. Light brown silt; 4. Limestone fragments.

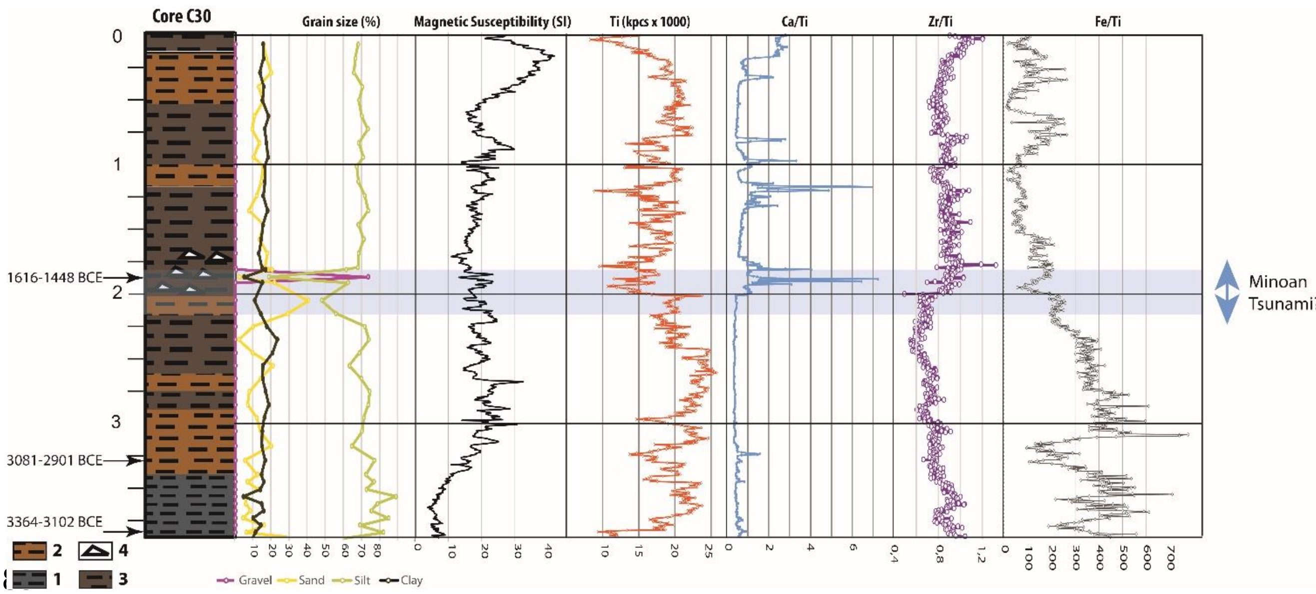

Fig. S11. Grain-size distribution of Sand beach sampled 30cm under the current beach surface

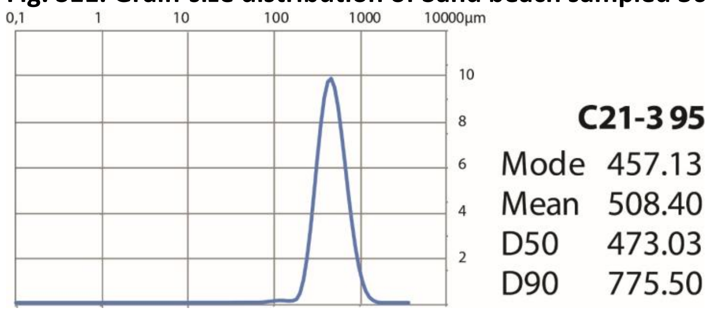

Fig. S12. Microfaunal analyses of samples from cores C20, C22, C26, C29, C30

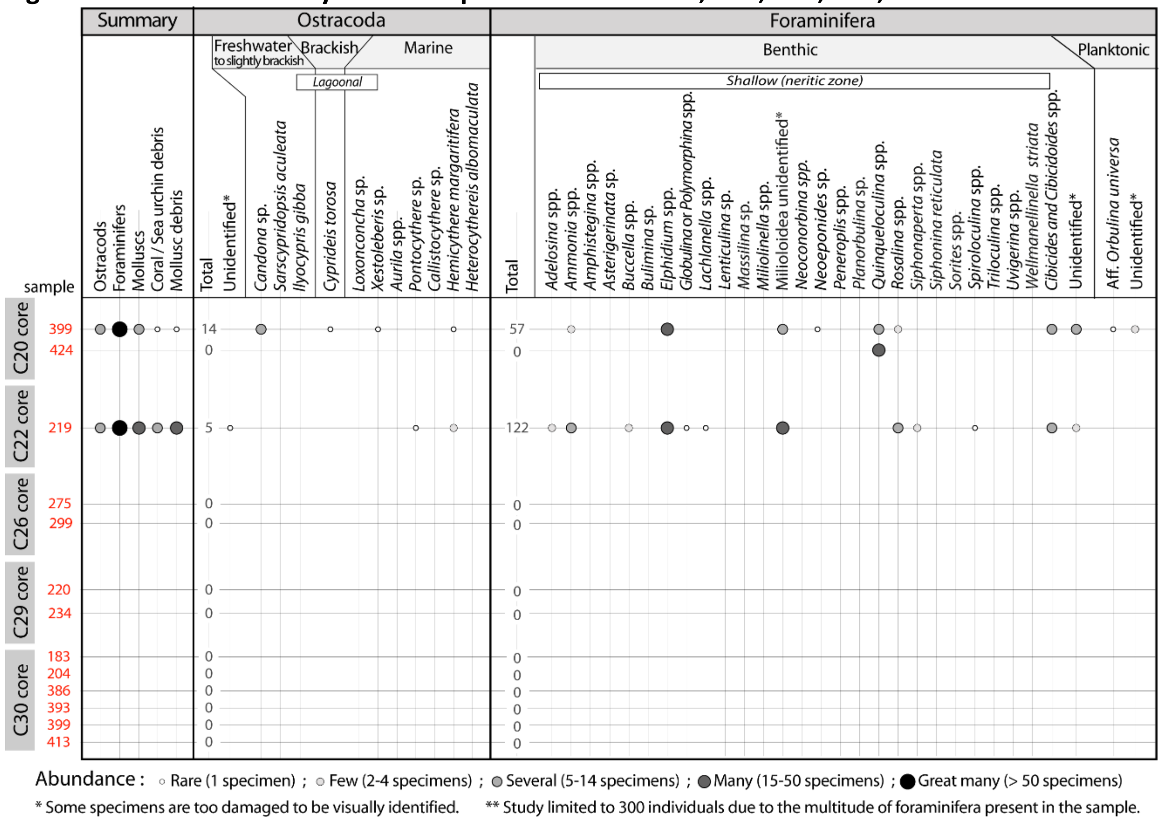

Fig. S13. Microphotographs of ostracods species identified in the samples of Malia cores C21, C20 & C22. 1. Aurila convexa, LV, external view; 2. Aurila prasina, LV, external view; 3. Aurila sp., LV, external view; 4. Bairdia sp., RV, external view; 5. Aff. Callistocythere sp., LV, external view. 6. Candona aff. angulata, LV, external view; 7. Candona sp., RV, internal view; 8. Candona sp., LV, external view; 9. Cyprideis torosa, LV, internal view; 10. Cyprideis torosa, LV, external view. 11. Cyprinotus salinus, RV, external view; 12. Hemicythere margaritifera, RV, internal view; 13. Hemicythere margaritifera, LV, external view; 14. Heterocythereis albomaculata, LV, external view; 15. Ilyocypris gibba, RV, internal view. 16. Ilyocypris gibba, RV, external view; 17. Loxoconcha sp., LV, external view.

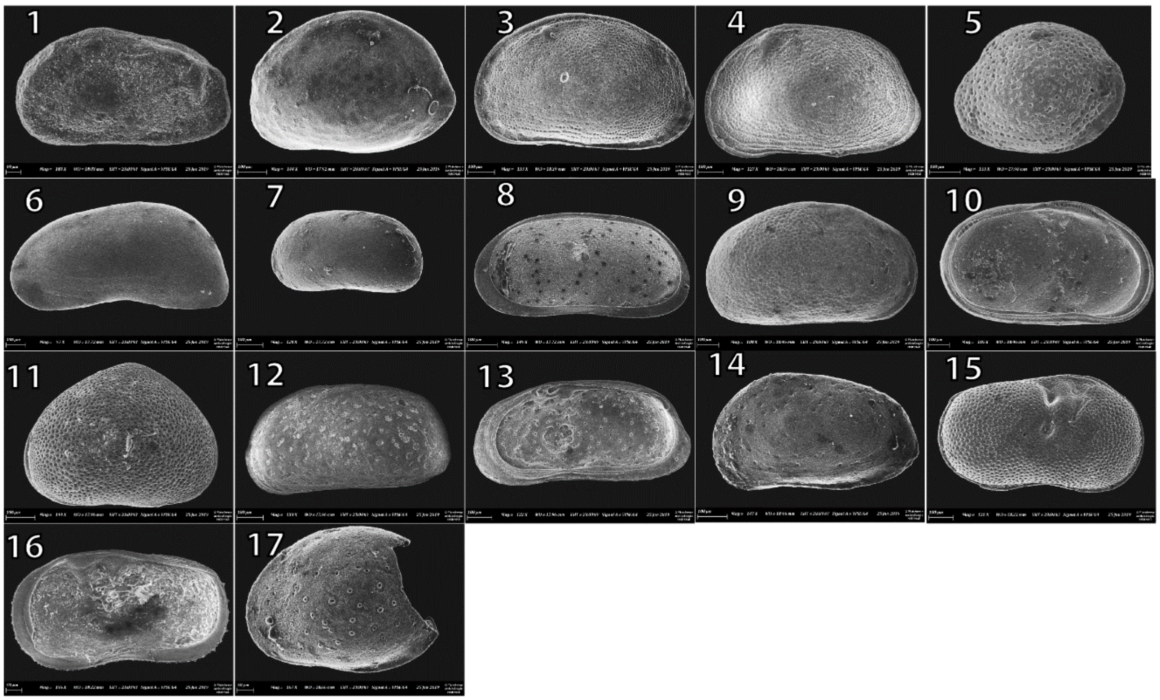

Fig. S14. Microphotographs of benthic foraminifera species (more than 4 individuals) for sample C21-U4c-299. 1. Ammonia spp.; 2. Elphidium spp.; 3. Cibicidoides lobatulus; 4. Elphidium crispum; 5. Quinqueloculina spp.; 6. Elphidium aff. Macellum; 7. Elphidium aff. Complanatum; 8. Cibicides refulgens; 9. Asterigerinata mamilla; 10. Buccella sp.; 11. Cibicidoides spp.; 12. Elphidium aff. Advenum; 13. Neoconorbina spp.; 14. Quinqueloculina aff. Stalkeri; 15. Elphidium aculeatum; 16. Rosalina spp.

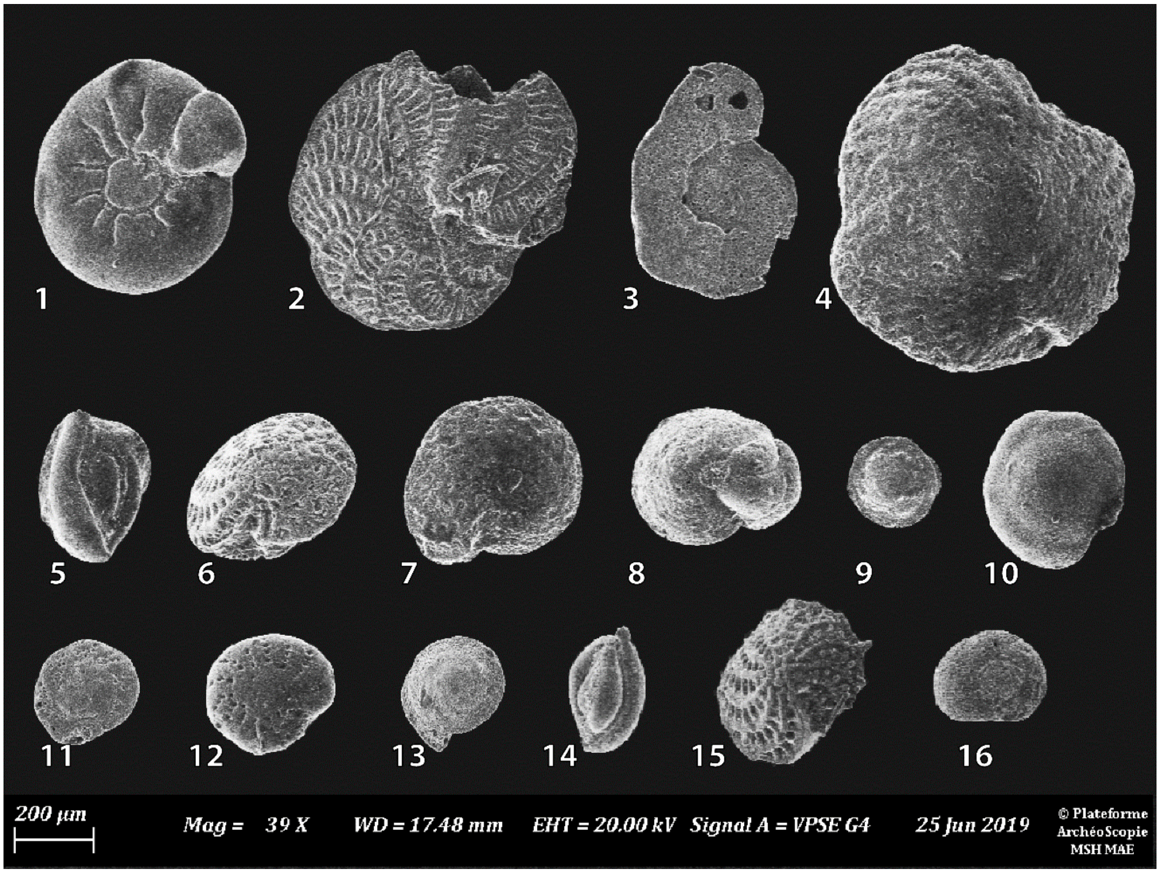

Fig. S15. Microphotographs of planktonic foraminifera species identified in sample C21-U4c-299. 1. Aff. Globorotalia menardii; 2. Aff. Neogloboquadrina sp.; 3. Aff. Neogloboquadrina sp.; 4. Aff. Orbulina sp; 5 to 15. Undetermined Globigerinitoidea or Globorotalioidea

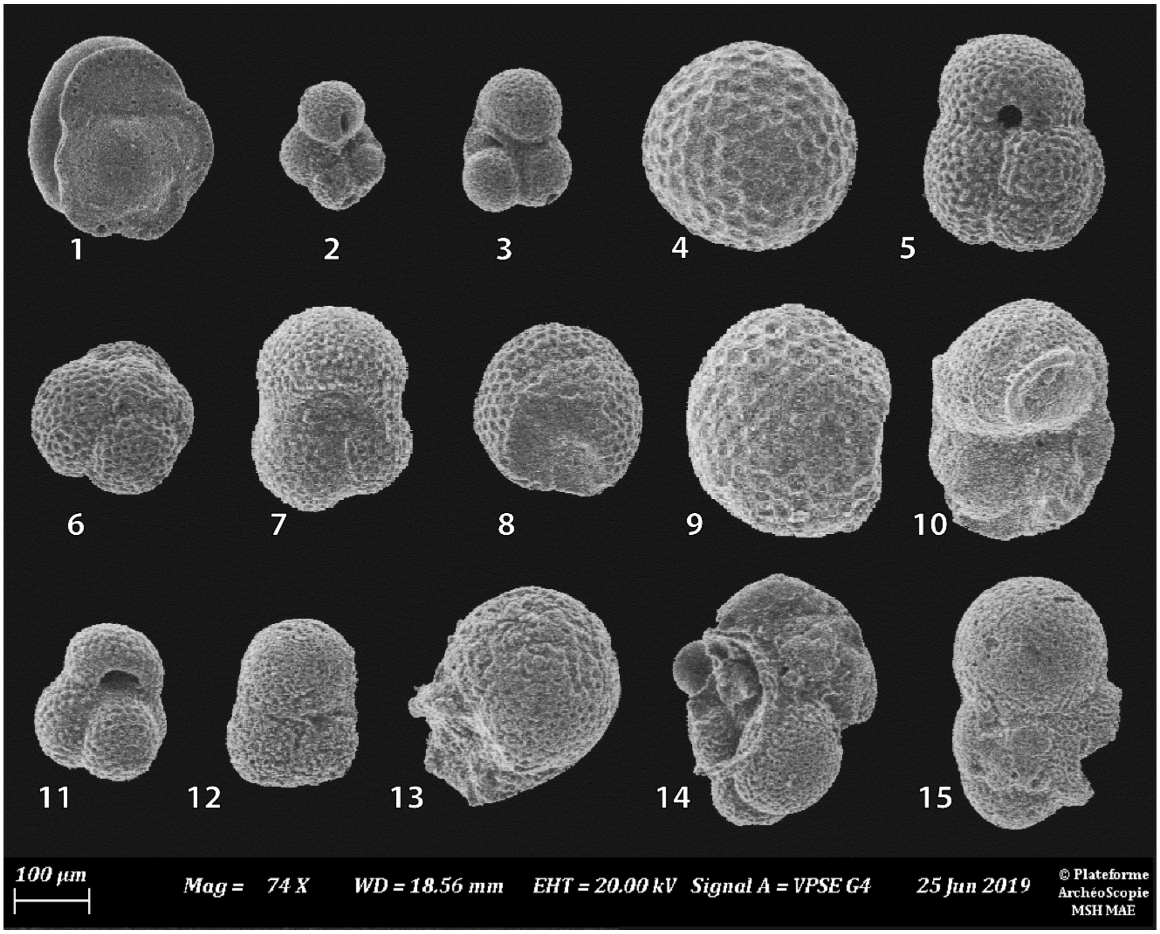

Fig. S16. Microphotographs of benthic foraminifera species (more than 2 individuals) and Cibicides aff. Kullenbergi of sample C21-U4b-320. 1. Cibicidoides lobatulus; 2. Ammonia sp.; 3. Elphidium crispum; 4. Elphidium aff. Complanatum; 5. Elphidium aff. Macellum; 6. Elphidium sp.; 7. Asterigerinata aff. Mamilla; 8. Rosalina aff. Bradyi; 9. Elphidium aff. Fichtelianum; 10. Cibicides sp.; 11. Rosalina aff. Obtuse; 12. Rosalina sp.; 13. Elphidium aff. Margaritaceum; 14. Cibicides aff. Kullenbergi.

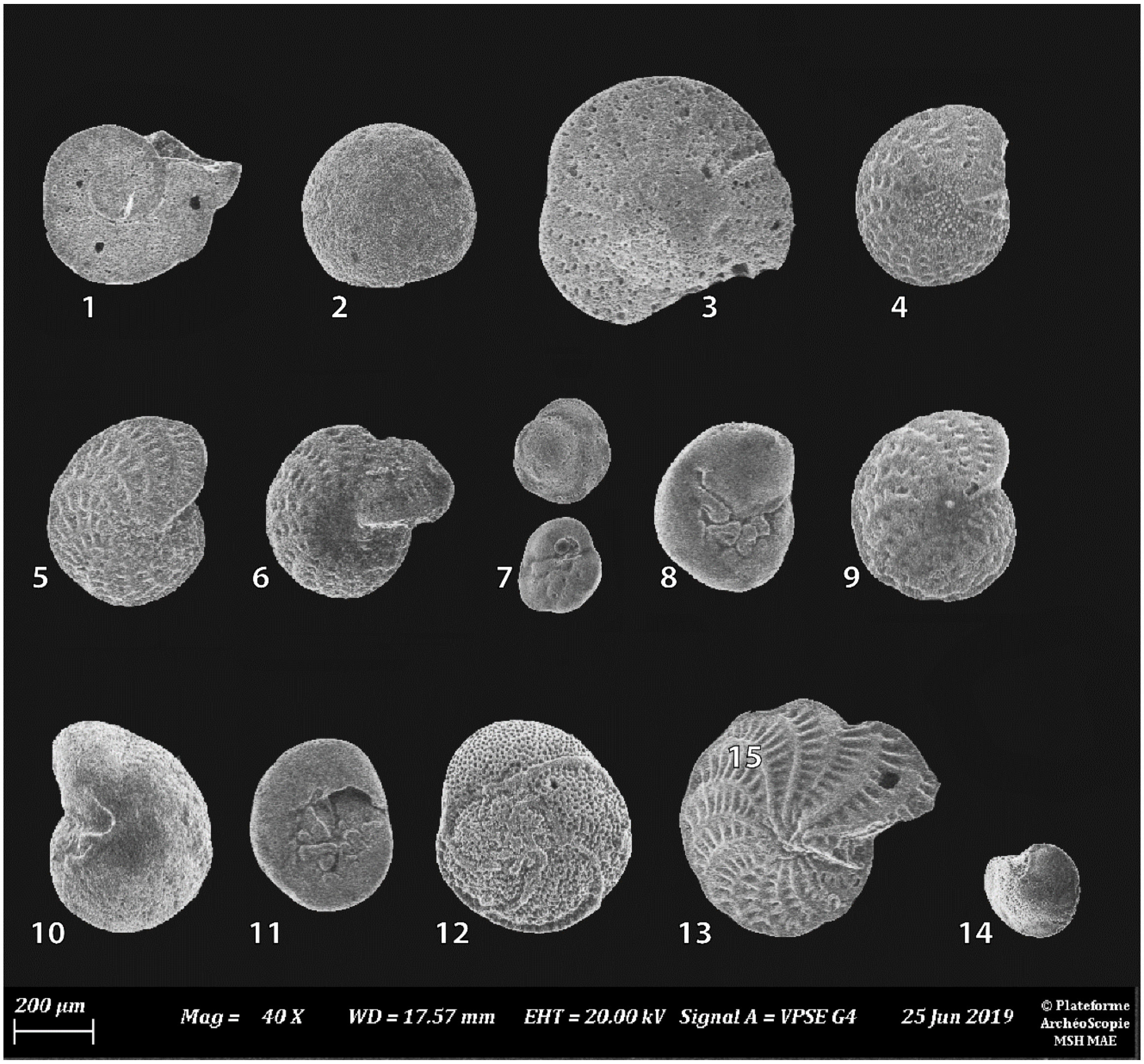

Table S1. Table of the radiocarbon dates obtained from the Malia marsh sedimentary archives *(in italic, rejected dating)*

Core	Depth (m)	Material	^{14}C Age	Error 2σ	Cal. 2σ	Sample Code	Reference
C6	2.00	Gyttja	536	35	1282-1490 CE	Lyon-7112	Lespez et al., 2003
C6	*2.18*	*Gyttja*	*1910*	*70*	*47 BCE-317 CE*	*Lyon-7113*	Lespez et al., 2003
C6	2.73	Gyttja	1770	55	133-413 CE	Lyon-7114	Lespez et al., 2003
C6	2.97	Gyttja	2020	70	337 BCE-203 CE	Lyon-7115	Lespez et al., 2003
C6	3.755	Gyttja	3340	50	1743-1505 BCE	Lyon-7116	Lespez et al., 2003
C6	4.04	Plant remain	3790	45	2448-2040 BCE	Lyon-7117	Lespez et al., 2003
C6	4.175	Charcoal	3955	50	2578-2293 BCE	Lyon-7118	Lespez et al., 2003
C6	4.83	Gyttja	5080	65	4037-3662 BCE	Lyon-7119	Lespez et al., 2003
C6	4.99	Gyttja	5210	55	4235-3819 BCE	Lyon-7120	*Lespez et al., 2003*
C6	*5.32*	*Plant remain*	*4765*	*165*	*3950-3094 BCE*	*Lyon-7121*	Lespez et al., 2003
C6	7.03	Gyttja	7440	80	6439-6088 BCE	Lyon-7122	Lespez et al., 2003
C28	1.11	Charcoal	1040	30	893-1114 CE	Poz-85400	This study
C28	*1.3*	*Charcoal*	*100.3*	*0.35pMC*	*Modern*	*Poz-85401*	*This study*
C28	3.00	Charcoal	3995	35	2623-2411 BCE	Poz-85441	This study
C28	*3.31*	*Charcoal*	*3800*	*35*	*2403-2062 BCE*	*Poz-85756*	*This study*
C28	3.8	Charcoal	4220	30	2905-2678 BCE	Beta-510919	This study
C28	4.16	Gyttja	4840	35	3702-3527 BCE	Poz-85757	This study
C28	4.31	Gyttja	5815	35	4782-4550 BCE	Poz-85759	This study
C26	1.255	Gyttja	585	30	1303-1416 CE	Poz-83103	This study
C26	1.875	Gyttja	1370	30	605-772 CE	Poz-83102	This study
C26	2.33	Gyttja	2015	30	95 BCE-109 CE	Poz-83104	This study
C26	2.825	Gyttja	3270	30	1616-1456 BCE	Poz-83106	This study
C26	3.275	Wood	3500	30	1919-1701 BCE	Poz-83107	This study
C26	3.94	Gyttja	4110	30	2867-2573 BCE	Poz-83108	This study
C26	4.295	Gyttja	5155	30	4045-3811 BCE	Poz-83109	This study
C26	4.825	Gyttja	5340	40	4324-4049 BCE	Poz-83110	This study
C26	5.435	Gyttja	5930	40	4932-4714 BCE	Poz-83111	This study
C26	5.715	Gyttja	6230	40	5306-5054 BCE	Poz-83112	This study
C30	1.94	Charcoal	3255	35	1613-1446 BCE	Poz-85336	This study
C30	*2.855*	*Charcoal*	*2825*	*30*	*1107-901 BCE*	*Poz-85338*	*This study*
C30	3.00	Charcoal	4520	30	3360-3101 BCE	Beta-480127	This study
C30	3.28	Charcoal	4350	30	3077-2899 BCE	Poz-85339	This study
C30	3.88	Charcoal	4535	35	3366-3101 BCE	Poz-85340	This study
C30	4.41	Charcoal	4500	35	3357-3041 BCE	Poz-85341	This study
C30	4.92	Charcoal	4480	30	3341-3031 BCE	Beta-451310	This study
C29	*2.985*	*Plant remain*	*4920*	*30*	*3769-3642 BCE*	*Beta-451311*	*This study*
C29	3.62	Gyttja	4690	30	3605-3370 BCE	Beta-451312	This study

C29	4.95	Charcoal	4720	30	3628-3375 BCE	Beta-451313	This study
C22	0.7	Charcoal	2000	80	197 BCE-218 CE	Poz-96172	This study
C22	1.24	Charcoal	3115	35	1492-1279 BCE	Poz-96173	This study
C22	2.11	Charcoal	3200	30	1513-1417 BCE	Poz-96175	This study
C20	2.67	Charcoal	3220	30	1533-1427 BCE	Poz-85442	This study
C21	1.16	Charcoal	210	420	Post 979 CE	Poz-96170	This study
C21	1.96	Charcoal	820	35	1168-1274 CE	Poz-96171	This study
C21	*2.86*	*Gyttja*	*4070*	*30*	*2850-2488 BCE*	*Poz-95029*	This study
C21	2.895	Gyttja	2585	30	811-592 BCE	Poz-105990	This study
C21	2.995	Charcoal	3490	35	1920-1694 BCE	Poz-105975	This study
C21	3.22	Charcoal	3425	35	1876-1622 BCE	Poz-105979	This study
C21	3.44	Gyttja	3380	35	1751-1540 BCE	Poz-95778	This study
C21	3.67	Gyttja	3800	35	2403-2062 BCE	Poz-95779	This study

Table S2. Table of the radiocarbon dates obtained from peat layer under the tephra deposits at Gölhisar lake

Site	Core	Depth (m)	Material	^{14}C Age	Error 2σ	Cal. 2σ	Sample Code	Reference
Gölhisar (Turkey)	GHA.92-3	0.59-0.63	Peat	3300	70	1674-1499	Beta-56673	Eastwood et al. 1999
Gölhisar (Turkey)	GHE-93-7	0.13-0.21	Peat	3225	45	1528-1441	SRR-5188	Eastwood et al. 1999

SI References

S1. Raban, A., Minoan and Canaanite harbours.Thalassa: l'Egée préhistorique et la mer, in: *Actes de la troisième Rencontre égéenne internationale de l'Université de Liège* (Aegaeum **7** 1991), pp. 129-146.

S2. Reimer, P. J., McCormac, F. G., Marine radiocarbon reservoir corrections for the Mediterranean and Aegean Seas. *Radiocarbon* **44** (1), 159-166 (2002)..

S3. Boaretto, E., Mienis, H. K., Sivan, D., Reservoir age based on pre-bomb shells from the intertidal zone along the coast of Israel. *Nuclear Instruments and Methods in Physics Research B* **268**, 966-968 (2010).

S4. Blaauw, M., and Christen, J. A. (2011), "Flexible paleoclimate age-depth models using an autoregressive gamma process," Bayesian Analysis, 6(3), 457–474.